Theory of the $d^{10}-d^{10}$ Closed-Shell Attraction. 4. $X(AuL)_n^{m+}$ Centered Systems

Pekka Pyykkö* and Toomas Tamm†

Department of Chemistry, PL 55 (A. I. Virtasen Aukio 1), FIN-00014, University of Helsinki, Finland

Received April 3, 1998

The title species with the central atoms C, N, O, P, and S and up to six $-AuPH_3$ ligands were studied at the MP2 level using effective core potentials. Structural parameters of the experimental systems were reproduced well. Two different ways of estimating the intramolecular gold−gold interaction energy from the calculated total energies are proposed, and the calculated interaction energies are found to correlate with the gold−gold distances in the systems. A giant proton binding energy of 1213 kJ/mol is calculated for the C_{4v} species $[HC(AuPH_3)_4]^+$.

1. Introduction

Intra- and intermolecular closed-shell interactions between heavy metal atoms, such as Au(I), can achieve a strength qualitatively comparable with strong hydrogen bonding. We have recently summarized the available theoretical and experimental evidence.[1]

Starting with the original observation[2] that this attraction comes from correlation effects and is absent at the Hartree−Fock (HF) level, we have presented increasing evidence for its long-distance R^{-6} dispersion nature, with some induction contributions. The technical requirements such as the basis sets, correlation methods, pseudopotentials, the particular metal M, and the role of relativity were also studied, especially in the two recent papers on free, perpendicular, model dimers.[3,4] In a third paper, ring systems were separately considered.[5]

We now address a class of compounds not previously considered at ab initio level, viz., the centered systems of the general type $[X(AuL)_n]^{m+}$. This class contains some of the unexpected new compounds, such as Schmidbaur's $[C(AuL)_6]^{2+}$,[6] thought to derive a part of its chemical stability from the "aurophilic" attraction between the six golds. So far, only density-functional theory (DFT) treatments exist for such compounds.[7−11] Although they are able to handle dynamic correlation, the current DFT methods are not able to handle dispersion effects in a treatment where the system is a single supermolecule. In another recent study,[12] similar five- and six-coordinated nitrogen, phosphorus, and arsenic ions have been studied by Rasul et al., using hydrogen atoms as model ligands. The work provided useful insight into the local minima on the corresponding potential energy surfaces, but the aurophilic attraction is obviously absent in these models.

At the semiempirical (CNDO/1) level, Boča has studied empty $(AuL)_n^{m+}$ gold clusters.[13] The influence of the particular ligand, L, on geometries and orbital energies has been discussed in his paper.

Thus the entire problem of determining aurophilic energies in centered systems at the ab initio level is fresh and new. As in the rings,[5] the primary chemical bonds already bring the interacting heavy metal atoms near each other, so particularly strong dispersion interactions can also be expected. The calculated structural data can be compared with a large class of experimentally known compounds.

2. Systems Studied

The studied systems correspond to the general formula $[Y_l-X-(AuL)_n]^{m+}$, where the central atom X is one of C, N, O, P, or S, and the apical ligand Y is either hydrogen or absent (the $-CN$ group was used as Y in one case). The ligand L is the $-PH_3$ (phosphine) group. For carbon as the central atom, all n values up to 6 were considered. For nitrogen, n up to 5 was investigated, and for the other central atoms, n was limited to 4. The choice of Y primarily followed the experimental data; the various bulky ligands were, however, modeled by hydrogen in most cases.

In the experimental structures, the ligand on the "back" side of the gold atoms is typically triphenylphosphine, $-P(C_6H_5)_3$. For computational efficiency, this

* E-mail: Pekka.Pyykko@helsinki.fi.
† E-mail: toomas@chem.helsinki.fi.

(1) Pyykkö, P. *Chem. Rev.* **1997**, *97*, 597.
(2) Pyykkö, P.; Zhao, Y. *Angew. Chem.* **1991**, *103*, 622; *Angew. Chem., Int. Ed. Engl.* **1991**, *30*, 604.
(3) Pyykkö, P.; Runeberg, N.; Mendizabal, F. *Chem. Eur. J.* **1997**, *3*, 1451.
(4) Pyykkö, P.; Mendizabal, F. *Chem. Eur. J.* **1997**, *3*, 1458.
(5) Pyykkö, P.; Mendizabal, F. *Inorg. Chem.* **1998**, *37*, 3018.
(6) Scherbaum, F.; Grohmann, A.; Huber, B.; Krüger, C.; Schmidbaur, H. *Angew. Chem.* **1988**, *100*, 1602; *Angew. Chem., Int. Ed. Engl.* **1988**, *27*, 1544.
(7) Rösch, N.; Görling, A.; Ellis, D. E.; Schmidbaur, H. *Angew. Chem.* **1989**, *101*, 1410. *Angew. Chem., Int. Ed. Engl.* **1989**, *28*, 1357.
(8) Görling, A.; Rösch, N.; Ellis, D. E.; Schmidbaur, H. *Inorg. Chem.* **1991**, *30*, 3986.
(9) Häberlen, O. D.; Chung, S.-C.; Rösch, N. *Int. J. Quantum Chem.* **1994**, *S28*, 595.
(10) Häberlen, O. D.; Schmidbaur, H.; Rösch, N. *J. Am. Chem. Soc.* **1994**, *116*, 8241.
(11) Chung, S.-C.; Krüger, S.; Schmidbaur, H.; Rösch, N. *Inorg. Chem.* **1996**, *35*, 5387.
(12) Rasul, G.; Prakash, G. K. S.; Olah, G. A. *J. Am. Chem. Soc.* **1997**, *119*, 12984.
(13) Boča, R. *J. Chem. Soc., Dalton Trans.* **1994**, 2061−2064.

10.1021/om980255+ CCC: $15.00
Publication on Web 10/08/1998

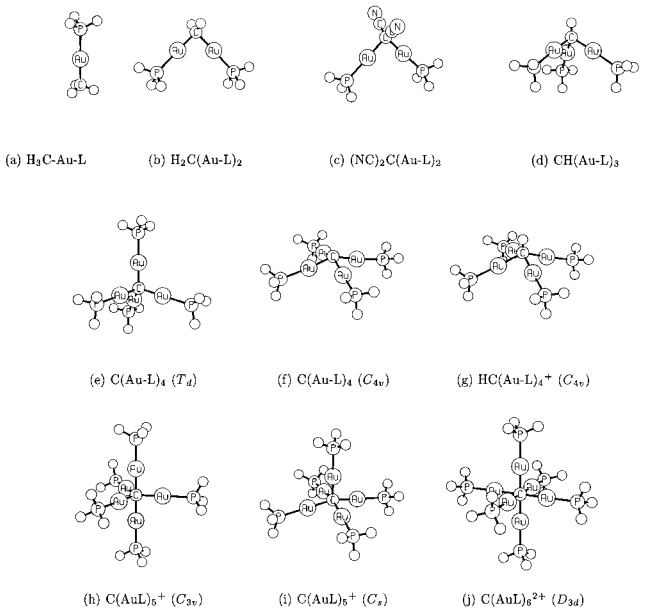

Figure 1. ORTEP[15] drawings of some of the systems studied.

Table 1. Overall and Approximate Framework Symmetries of Some of the Systems

example	symmetry: total	symmetry: CAu_n	notes
$CH_2(AuL)_2$	C_{2v}	C_{2v}	
$CH(AuL)_2^-$	C_s	C_{2v}	H is out of Au−C−Au plane.
$CH(AuL)_3$	C_{3v}	C_{3v}	
$C(AuL)_4$	T_d	T_d	Preferred symmetry for the $X(AuL)_4$ systems is discussed below.
$C(AuL)_4$	C_{4v}	C_{4v}	
$C(AuL)_5^+$	C_{3v}	D_{3h}	Equatorial $-PH_3$ deletes σ_h plane.
$C(AuL)_5^+$	C_s	C_{4v}	Apical $-PH_3$ deletes C_4 axis.
$C(AuL)_6^{2+}$	D_{3d}	O_h	Terminal $-PH_3$ deletes C_4 axes.

was replaced by the unsubstituted phosphine group, $-PH_3$. This substitution has been found to have little influence on the X-Au and Au−P bond lengths,[14] while permitting the calculations of larger systems within reasonable computational effort.

For the bridged systems with two gold atoms (referred to as "A-frames" below), C_{2v} symmetry was assumed, unless the asymmetry of the −Y group(s) dictated C_s. The systems containing three golds ("tripods") were studied with C_{3v} symmetry. The $n = 4$ case can assume either ammonium-like T_d, distorted tetrahedral C_{3v}, or pyramidal, "tetrapod", C_{4v} symmetries. All three possibilities were investigated.

The geometries of the systems with five gold atoms were limited to C_{3v} (distorted D_{3h} due to the asymmetry of the equatorial $-PH_3$ ligands) and C_{4v} point groups. The only six-gold system was calculated assuming D_{3d} symmetry (approximate O_h for the carbon−gold subsystem). Geometries of some representative carbon-centered systems are illustrated in Figure 1. The symmetries of the frameworks, as well as the whole molecules, are summarized in Table 1.

3. Method

Basis Sets and Pseudopotentials. For gold, we used the small-core pseudorelativistic Stuttgart effective core potential (ECP) and the corresponding basis set,[16] augmented with two ($\alpha = 0.2$ and $\alpha = 1.19$) f-type polarization sets. The motivation behind this choice has been discussed in the previous papers of this series.[3−5]

Table 2. Basis Sets and Effective Core Potentials (ECPs) Used in this Work

element	basis	ECP	exponents of polarization functions	refs
H	(4s 1p)/[2s 1p]		$\alpha_p = 0.8$	19
C	(4s 4p 1d)/[2s 2p 1d]	Bergner	$\alpha_d = 0.80$[a]	17, 18
N	(4s 4p 1d)/[2s 2p 1d]	Bergner	$\alpha_d = 0.864$	17, 18
O	(4s 5p 1d)/[2s 2p 1d]	Bergner	$\alpha_d = 1.154$	17, 18
P	(4s 4p 1d)/[2s 2p 1d]	Bergner	$\alpha_d = 0.34$	17, 18
S	(4s 5p 1d)/[2s 2p 1d]	Bergner	$\alpha_d = 0.421$	17, 18
Au	(8s 7p 6d 2f)/[6s 5p 3d 2f]	Andrae	$\alpha_f = 1.19, 0.2$	16

[a] In ref 18 the value of 0.6 is recommended instead.

For the second- and third-row elements the relativistic Stuttgart pseudopotentials and corresponding basis sets[17] were employed. Where the original basis sets were contracted, the most diffuse primitive of each *l*-value was decontracted to obtain split-valence quality. One set of *d*-type polarization functions, with exponents chosen from Huzinaga,[18] was added at each atom. For hydrogen, we used the Huzinaga 4s basis set,[19] decontracted for double-ζ quality and augmented with a set of p polarization functions with $\alpha = 0.8$.

The basis sets and effective core potentials used in this work are summarized in Table 2.

Electron Correlation. All calculations were performed at Hartree−Fock and second-order Møller−Plesset perturbation theory (MP2) levels. Since it has been suggested[2] that aurophilic attraction is primarily a correlation effect, the Hartree−Fock calculations provide a convenient way of "turning off" the attraction, while still providing reasonable approximations for the overall geometric structure of the systems.

The sensitivity of the geometry to the correlation method was investigated by varying the Au−S−Au angle in $S(Au-L)_2$ while keeping the other geometric parameters at the values of the MP2-optimized geometry. The resulting minima of Au···Au distances are plotted in Figure 2. From these results we concluded that the MP2 method may actually somewhat exaggerate the aurophilic attraction (as also noted in ref 3). The first noticeably more accurate method, CCSD, would have been prohibitively expensive for a study of this magnitude, however.

To gain additional speedup, the resolution of identity MP2[20−22] (RI-MP2) methodology was used in the geometry optimizations of the larger systems. In the RI-MP2 approximation, the products of basis functions are

(14) Häberlen, O. D.; Rösch, N. *J. Phys. Chem.* **1993**, *97*, 4970.
(15) ORTEP-III: Oak Ridge Thermal Ellipsoid Plot program for crystal structure illustrations. Burnett, M. N.; Johnson, C. K. Oak Ridge National Laboratory Report ORNL-6895; http://www.ornl.gov/ortep/ortep.html, 1996.
(16) Andrae, D.; Häussermann, U.; Dolg, M.; Stoll, H.; Preuss, H. *Theor. Chim. Acta (Berlin)* **1990**, *77*, 123.
(17) Bergner, A.; Dolg, M.; Köchle, W.; Stoll, H.; Preuss, H. *Mol. Phys.* **1993**, *80*, 1431.
(18) Huzinaga, S., Ed. *Gaussian Basis Sets for Molecular Calculations*; Number 16 in Physical Sciences Data; Elsevier: Amsterdam, 1984.
(19) Huzinaga, S. *J. Chem. Phys.* **1965**, *42*, 1293.
(20) Feyereisen, M.; Fitzgerald, G.; Komornicki, A. *Chem. Phys. Lett.* **1993**, *208*, 359.
(21) Vahtras, O.; Almlöf, J.; Feyereisen, M. W. *Chem. Phys. Lett.* **1993**, *213*, 514.
(22) Weigend, F.; Häser, M. *Theor. Chim. Acta (Berlin)* **1997**, *97*, 331.

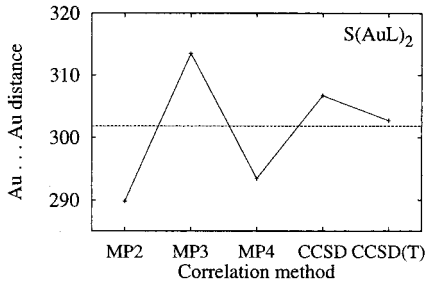

Figure 2. Dependence of the calculated Au···Au distance for $S(AuPH_3)_2$ on the correlation method. The dashed line is the experimental distance for $S(AuPPh_3)_2$.

Table 3. Exponents of the Auxiliary Basis Sets Used in this Work: All Auxiliary Basis Sets were Even-Tempered (Ratio = 3.0) and Fully Uncontracted

element	*l*-value	no. of functions	highest exponent	lowest exponent
H	s	6	26.723 000 0	0.109 971 2
	p	6	14.161 500 0	0.058 277 8
	d	2	1.600 000 0	0.533 333 3
C	s	5	4.526 202 0	0.055 879 0
	p	5	10.646 126 0	0.131 433 7
	d	6	16.766 050 0	0.068 996 1
	f	5	9.183 025 0	0.113 370 7
O	s	7	94.211 036 0	0.129 233 2
	p	8	63.797 737 0	0.029 171 3
	d	7	48.259 518 0	0.066 199 6
	f	7	17.846 219 0	0.024 480 4
N	s	7	65.313 678 0	0.089593 5
	p	6	44.803 813 0	0.184 377 8
	d	6	33.520 839 0	0.137 945 8
	f	5	13.010974 0	0.160 629 3
P	s	6	13.444 616 0	0.055 327 6
	p	6	8.005 529 0	0.032 944 6
	d	6	7.062 308 0	0.029 063 0
	f	4	1.623221 0	0.060 119 3
S	s	6	13.667 036 0	0.056 242 9
	p	7	8.650 657 0	0.011866 5
	d	7	7.254 518 0	0.009 951 3
	f	5	2.238 139 0	0.027 631 3
Au	s	9	40.230 598 0	0.006 131 8
	p	8	28.724 964 0	0.013 134 4
	d	8	24.259 248 0	0.011 092 5
	f	8	21.305 299 0	0.009 741 8
	g	8	21.115 299 0	0.009 654 9
	h	7	9.609 665 0	0.013 182 0

expanded in an auxiliary basis set $\{\gamma_u\}$:

$$\chi_p(r)\,\chi_q(r) \approx \sum_u C_u^{pq}\gamma_u \qquad (1)$$

Such auxiliary basis sets were generated as even-tempered ones, i.e., with exponents $\alpha_i = \alpha_0\beta^i$, with a factor β of 3.0; see Table 3. The range of exponents for each angular momentum was chosen to cover the whole range of possible sums of the exponents of the primary basis functions which are capable of yielding density expressible with auxiliary functions of the particular *l*-value. No contractions were used in the auxiliary basis set. The resulting exponents are given in Table 3.

For benchmarking, the C-centered systems with up to three gold atoms were also optimized at the non-RI-MP2 level. The speedup for the RI-MP2 method was approximately 2 times, compared to the regular MP2. Larger speedups have been reported earlier[22] when smaller auxiliary basis sets were used. The accuracy in geometries was better than ±1 pm and ±1 deg and 5 kJ/mol in total energies.

For all systems optimized at the RI-MP2 level, regular MP2 single-point calculations were performed at the final optimized geometries. The resultant energies were compared to the respective RI-MP2 ones. The differences were less than 10 kJ/mol in all cases. The reported energies in this paper are all from the respective classical MP2 calculations; no RI-MP2 energies were used in the estimates of aurophilic attraction energies below.

Geometry Optimization. Geometries were optimized at each level of approximation within the constraints of the appropriate (C_s, C_{2v}, C_{3v}, C_{4v}, or T_d) symmetries. If the rotation of the terminal $-PH_3$ ligands would have broken the symmetry, their dihedral angle was fixed. The validity of this assumption was tested on the $CH_2(Au-L)_2$ system, where the rotational barriers of the terminal $-PH_3$ groups were found to be less than 0.25 kJ/mol at the MP2 level.

Software. The calculations were performed with the Turbomole[23,24] program package; version 4.5 obtained from the authors was used. Gaussian 94[25] was used in preparation of some of the input files, for calculation of some smaller systems, and for consistency checks. ACES II[26] was used for the MP3, MP4, and coupled cluster calculations.

The latest versions (4.5 and up) of Turbomole can calculate analytic derivatives for geometry optimizations even when f-functions and ECPs are used simultaneously. Such capability is missing from many other current codes, including all others at our disposal. Analytic derivatives at the RI-MP2 level[22] are another recent addition to Turbomole, which enabled these calculations to be performed at a reasonable computational cost.

4. Results and Discussion

4.1. Subsection Structures. The optimized geometries and total energies are reported in Tables 4−10. It is immediately evident that wherever the symmetry is not restricting the bending of Au−X−Au angles, the gold−gold distances, compared to the Hartree−Fock ones, are significantly shortened at the MP2 level. The Au−P distances are also shortened by correlation effects. The other bond lengths are almost unchanged or slightly lengthened, as expected from MP2 calculations.

(23) Ahlrichs, R.; Bär, M.; Häser, M.; Horn, H.; Kölmel, C. *Chem. Phys. Lett.* **1989**, *162*, 165.

(24) Ahlrichs, R.; von Arnim, M. In *Methods and Techniques in Computational Chemistry/METECC-95*; Clementi, E.; Corongiu, G., Eds.; Club Européen MOTECC, 1995; Chapter 13, pp 509−554.

(25) Frisch, M. J.; Trucks, G. W.; Schlegel, H. B.; Gill, P. M.; Johnson, B. G.; Robb, M. A.; Cheeseman, J. R.; Keith, T. A.; Peterson, G. A.; Montgomery, J. A.; Raghavachari, K.; Al-Laham, M. A.; Zakrzewski, V. G.; Ortiz, J. V.; Foresman, J. B.; Cioslowski, J.; Stefanov, B. B.; Nanayakkara, A.; Challacombe, M.; Peng, C. Y.; Ayala, P. Y.; Chen, W.; Wong, M. W.; Andres, J. L.; Replogle, E. S.; Gomperts, R.; Martin, R. L.; Fox, D. J.; Binkley, J. S.; Detrees, D. J.; Baker, J.; Stewart, J. P.; Head-Gordon, M.; Gonzalez, C.; Pople, J. *Gaussian 94*; Gaussian, Inc.: Pittsburgh, PA, 1995.

(26) Stanton, J. F.; Gauss, J.; Watts, J. D.; Nooijen, M.; Oliphant, N.; Perera, S. A.; Szalay, P. G.; Lauderdale, W. J.; Gwaltney, S. R.; Beck, S.; Balková, A.; Bernholdt, D. E.; Baeck, K.-K.; Rozyczko, P.; Sekino, H.; Hober, C.; Bartlett, R. J. *ACES II:* a program product of the Quantum Theory Project, University of Florida. Integral packages included are VMOL (Almlöf, J.; Taylor, P. R.); VPROPS (Taylor, P.); ABACUS (Helgaker, T.; Jensen, H. J. Aa.; Jørgensen, P.; Olsen, J.; Taylor, P. R.).

Table 4. Basis Set Sizes and Total Energies of the Systems Studied (in Hartrees)

system	no. of basis functions	Hartree–Fock geometry		MP2 geometry	
		HF energy	MP2 energy	HF energy	MP2 energy
CH_3^-	28	−7.122 151	−7.281 552	−7.121 936	−7.281 733
CH_4	33	−7.838 733	−7.998 600	−7.838 622	−7.998 708
CH_3AuL	106	−150.161 588	−150.931 905	−150.158 535	−150.935 074
$CH(AuL)_2^-$	174	−291.805 461	−293.259 810	−291.789 756	−293.272 826
$CH_2(AuL)_2$	179	−292.482 133	−293.884 894	−292.471 147	−293.896 241
$(NC)_2C(AuL)_2$	221	−321.817 457	−323.719 405	−321.796 385	−323.740 076
$CH(AuL)_3$	252	−434.807 493	−436.861 623	−434.784 203	−436.883 689
$C(AuL)_4$ (T_d)	325	−577.140 890	−579.862 128	−577.123 375	−579.880 915
$C(AuL)_4$ (C_{3v})	325	−577.140 931	−579.862 158	−577.121 213	−579.881 096
$C(AuL)_4$ (C_{4v})	325	−577.099 458	−579.841 420	−577.074 496	−579.863 355
$CH(AuL)_4^+$	330	−577.629 748	−580.298 935	−577.605 673	−580.325 284
$C(AuL)_5^+$ (C_{3v})	403	−719.976 102	−723.322 603	−719.947 194	−723.354 654
$C(AuL)_5^+$ (C_s)	403	−719.973 029	−723.319 315	−719.936 564	−723.353 718
$C(AuL)_6^{2+}$ (D_{3d})	481	−862.689 125	−866.664 798	−862.643 350	−866.716 417
NH_3	28	−11.462 976	−11.647 279	−11.462 293	−11.647 919
NH_4^+	33	−11.813 120	−11.996 815	−11.812 480	−11.997 433
NH_2AuL	101	−153.789 982	−154.585 689	−153.786 844	−154.589 230
NH_3AuL^+	106	−154.229 727	−154.997 325	−154.225 832	−155.001 960
$NH(AuL)_2$	174	−296.109 183	−297.540 688	−296.097 580	−297.552 772
$NH_2(AuL)_2^+$	179	−296.599 523	−297.978 128	−296.587 114	−297.989 109
$N(AuL)_3$	247	−438.431 000	−440.522 711	−438.405 855	−440.548 395
$NH(AuL)_3^+$	252	−438.946 346	−440.963 650	−438.924 114	−440.981 074
$N(AuL)_4^+$ (T_d)	325	−581.284 952	−583.968 476	−581.269 72	−583.984 560
$N(AuL)_4^+$ (C_{3v})	325	−581.284 973	−583.968 456	−581.269 746	−583.984 525
$N(AuL)_4^+$ (C_{4v})	325	−581.237 396	−583.939 860	−581.210 684	−583.963 953
$N(AuL)_5^{2+}$ (C_{3v})	403	−723.967 629	−727.275 827	−723.940 583	−727.305 636
H_2O	23	−16.925 053	−17.076 041	−16.924 225	−17.076 824
H_3O^+	28	−17.197 132	−17.351 006	−17.195 292	−17.353 050
H_4O^{2+}	33	−17.104 738	−17.272 633	−17.104 620	−17.272 750
OHAuL	96	−159.258 451	−160.025 261	−159.254 455	−160.029 655
OH_2AuL^+	101	−159.662 887	−160.393 527	−159.654 587	−160.403 519
OH_3AuL^{2+}	106	dissociates			
$O(AuL)_2$	169	−301.575 498	−302.989 292	−301.565 014	−303.000 802
$OH_2(AuL)_2^{2+}$	179	−302.271 589	−303.572 229	−302.247 211	−303.598 562
$O(AuL)_3^+$	247	−444.400 038	−446.390 829	−444.366 313	−446.415 711
$O(AuL)_4^{2+}$ (T_d)	325	−587.083 321	−589.675 820	−587.064 442	−589.696 655
$O(AuL)_4^{2+}$ (C_{3v})	325	−587.083 318	−589.675 807	−587.064 053	−589.696 586
SH_2	23	−11.148 196	−11.269 111	−11.148 101	−11.269 197
SHAuL	96	−153.527 288	−154.251 078	−153.523 801	−154.255 305
SH_2AuL^+	101	−153.888 267	−154.597 688	−153.883 513	−154.603 257
$S(AuL)_2$	169	−295.896 727	−297.245 060	−295.883 659	−297.259 919
$S(AuL)_3^+$	247	−438.710 828	−440.644 379	−438.675 196	−440.679 769
$S(AuL)_4^{2+}$ (T_d)	325	−581.403 953	−583.916 580	−581.383 160	−583.939 789
$S(AuL)_4^{2+}$ (C_{3v})	325	−581.403 978	−583.916 548	−581.363 089	−583.940 864
$S(AuL)_4^{2+}$ (C_{4v})	325	−581.371 263	−583.909 453	−581.331 237	−583.958 463
PH_3	28	−8.109 320	−8.238 551	−8.109 090	−8.238 762
PH_2AuL	101	−150.474 024	−151.209 115	−150.471 093	−151.212 687
PH_3AuL^+	106	−150.866 264	−151.580 155	−150.862 852	−151.584 420
$PH_2(AuL)_2^+$	179	−293.273 491	−294.592 390	−293.265 186	−294.601 167
$PH(AuL)_3^+$	252	−435.661 346	−437.600 600	−435.647 004	−437.615 239
$P(AuL)_4^+$ (T_d)	325	−578.040 682	−580.616 489	−578.022 665	−580.636 317
$P(AuL)_4^+$ (C_{3v})	325	−578.040 710	−580.616 481	−577.998 822	−580.639 603
$P(AuL)_4^+$ (C_{4v})	325	−578.008 493	−580.626 858	−577.975 409	−580.665 461
$PH(AuL)_4^{2+}$ (C_{4v})	330	−578.331 961	−580.878 439	−578.292 822	−580.918 034

Influence of Aurophilic Attraction on Symmetry. For the systems with four and five groups around the central atom, different geometrical arrangements of these groups are possible. In the majority of ML_n systems encountered in chemistry, a tetrahedral arrangement is preferred for $n = 4$, and trigonal bipyramids are typical for $n = 5$.

However, when attractive forces are present between the ligand groups, such as is the case here, the tetrahedral symmetry may be lowered either to C_{3v}, yielding three short and three long Au–Au distances, or to C_{4v}, resulting in four Au–Au distances shorter than in the tetrahedron, and two longer diagonal ones. In the five-ligand case, a C_{4v} arrangement of the ligands may again be preferred over the C_{3v} structure. Experimentally, such slight symmetry breaking has been observed in crystals for $N(AuL)_4^+$ (C_{3v} symmetry[27,28]). Substantial deviations from the highest symmetry have been observed in $S(AuL)_4^{2+}$ (C_{4v} symmetry[29]) and $P(AuL)_5^{2+}$ (C_{4v} symmetry[30]). The species $C(AuL)_5^+$ and $N(AuL)_5^{2+}$ are (distorted) D_{3h},[31,32] and $O(AuL)_4^{2+}$ is T_d.[33]

(27) Slovokhotov, Y. L.; Struchkov, Y. T. *J. Organomet. Chem.* **1984**, *277*, 143.
(28) Zeller, E.; Beruda, H.; Kolb, A.; Bissinger, P.; Riede, J.; Schmidbaur, H. *Nature* **1991**, *352*, 141.
(29) Canales, F.; Gimeno, M. C.; Jones, P. G.; Laguna, A. *Angew. Chem.* **1994**, *106*, 811; *Angew. Chem., Int. Ed. Engl.* **1994**, *33*, 769.
(30) Backman, R. E.; Schmidbaur, H. *Inorg. Chem.* **1996**, *35*, 1399.
(31) Scherbaum, F.; Grohmann, A.; Müller, G.; Schmidbaur, H. *Angew. Chem.* **1989**, *101*, 464; *Angew. Chem., Int. Ed. Engl.* **1989**, *28*, 463.
(32) Grohmann, A.; Riede, J.; Schmidbaur, H. *Nature* **1990**, *345*, 140.
(33) Schmidbaur, H.; Hofreiter, S.; Paul, M. *Nature* **1995**, *377*, 503.

Table 5. Main Geometric Parameters of the Carbon-Centered Systems (in pm and deg)

system	method	C−Au bond	Au···Au distance	Au−P bond	Au−C−Au angle	C−Au−P angle
CH_3AuL	HF	209.7		242.3		180.0
	RI-MP2	203.6		233.1		180.0
	MP2	203.6		233.1		180.0
$CH(AuL)_2^-$	HF	199.3	346.5	237.1	120.75	179.8
	RI-MP2	197.0	286.5	231.1	93.32	176.2
$CH_2(AuL)_2$	HF	208.8	340.7	242.4	109.35	179.8
	MP2	202.7	294.7	232.7	93.30	178.3
	RI-MP2	202.7	294.0	232.6	93.03	178.3
$Ph_3PCH[Au(PPh_3)]_2^+$	expt[35]	207.6	299.8	226.8	92.5	177.4
$(NC)_2C(AuL)_2$	HF	213.5	338.2	239.0	104.73	179.0
	RI-MP2	205.2	292.7	230.1	90.98	179.6
	MP2	205.3	293.3	230.1	91.21	179.6
$(NC)_2C(AuPPh_3)_2$	expt[48]	210.1	291.2	226.8	87.7	174.3
$CH(AuL)_3$	HF	207.5	336.4	241.6	108.34	179.7
	MP2	201.1	295.3	231.4	94.48	177.1
	RI-MP2	201.0	294.6	231.4	94.24	177.0
$Me_3PC(AuPPh_3)_3^+$	expt[49]	205.7	317.7	228.3	101.0	174.8
$C(AuL)_4$ (C_{3v})	HF			turns into T_d		
	RI-MP2	195.9[a]	334.4[b]	230.4[a]	116.2[b]	180.0[a]
		197.9[c]	307.4[d]	230.8[c]	101.9[d]	179.5[c]
$C(AuL)_4$ (T_d)	HF	205.9	336.3	240.2	109.5	180.0
	RI-MP2	196.9	321.6	230.8	109.5	180.0
$C(AuL)_4$ (C_{4v})	HF	208.4	294.8	236.6	90.0	180.0
	RI-MP2	205.0	276.6	229.2	84.9	174.2
$CH(AuL)_4^+$	HF	217.5	297.5	240.7	86.3	177.2
	RI-MP2	209.7	278.4	231.0	83.2	177.4
$CH(AuPPh_3)_4^+$	expt[35]	212.5	280.3	227.6	82.6	172.4
$C(AuL)_5^+$ (C_{3v})	HF	216.3[a]	303.5[b]	239.0[a]	90.0[b]	180.0
		212.9[c]	368.7[d]	240.9[c]		120.0[e]
	RI-MP2	205.3[a]	288.3[b]	229.4[a]	90.0[b]	180.0
		202.4[c]	350.6[d]	231.3[c]	120.0[d]	
$C(AuPPh_3)_5^+$	expt[31]	208.7[a]	294.5[b]	226.3[a]	91.8[b]	
		207.9[c]	360.0[d]	229.0[c]	119.9[d]	173.0[a]
$C(AuL)_5^+$ (C_s)	HF	210.2[a]	336.2[e,f]	241.4[a]	104.1[e,f]	179.8[a]
		215.9[e,g]	296.1[e,g]	239.8[g]	86.6[e,g]	178.0[e,g]
	RI-MP2	203.4[a]	300.6[e,f]	232.4[a]	95.2[e,g]	179.9[a]
		203.8[e,g]	287.0[e,g]	229.7[e,g]	89.5[e,g]	179.6[e,g]
$C(AuL)_6^{2+}$ (D_{3d})	HF	220.7	312.1	240.3	90.0	180.0
	RI-MP2	207.3	293.1	230.8	90.0	179.9
$C(AuPPh_3)_6^{2+}$	expt[6]	212.5	300.4	227.2		174.4

[a] Axial. [b] Axial to equatorial. [c] Equatorial. [d] Between two equatorial Au atoms. [e] Average for symmetry-nonequivalent sites. [f] Axial to nonaxial. [g] Nonaxial.

The calculated results agree with the experiments for $C(AuL)_5^{2+}$, $O(AuL)_4^{2+}$, and $S(AuL)_4^{2+}$, while for $N(AuL)_4^+$ the calculated results prefer undistorted T_d symmetry over C_{3v}. The energetic cost of this distortion appears to be very small, however, and the discrepancy could be explained by crystal forces in the experimental system. We also predict that for $P(AuL)_4^+$ there should exist a clear preference of C_{4v} over C_{3v}, which is in turn preferred over T_d. The relative energies are 0, +68 kJ/mol, and +77 kJ/mol, respectively.

For completeness, we also calculated the relative stabilities of $As(AuL)_4^+$ at C_{4v} and T_d symmetries. This system has been studied earlier[34] using a smaller basis set. The qualitative results of the earlier study were reconfirmed: the C_{4v} is lower than T_d. Quantitatively, the energetic difference between the two symmetries was found to be 125.3 kJ/mol, a minor change from the 132.3 kJ/mol of the previous work.

Comparisons with Experimental Geometries. The available experimental structural data are included in Tables 4−10. Averaged crystallographic distances are given for slightly distorted systems. It should be mentioned that the experimental L groups are typically $-PPh_3$ instead of $-PH_3$. Similarly, in capped tripods and tetrapods, the experimental capping group Y, such as $-OSiMe_3$, was replaced by hydrogen for the calculations.

The $(NC)_2C(AuL)_2$ structure has both C−Au, Au···Au, and Au−P distances within a few picometers from experiment. The Au−C−Au angle is nearly tetrahedral at the HF level and diminishes to 91° at the MP2 level (expt 87.7°). In this case the molecular crystal and the model only differ in having different phosphines and the system is neutral.

The $CH(AuL)_3$ also is nearly tetrahedral at the HF level. The C_{3v} distortion is slightly exaggerated at the MP2 level, compared to experiment. Note that the apical groups Y are chemically different in the assumed model and in the experiment: −H and $-PPh_3$, respectively.

The "gilded methane", $C(AuL)_4$, shows three minima at the MP2 level: C_{3v}, T_d, and C_{4v}. The relative energies are 0, +0.5, and +46 kJ/mol, respectively. Thus there is no energetic cost (within the accuracy of this calculation) for the tetrahedral structure to distort into C_{3v}, and the pyramidal C_{4v} isomer is not prohibitively high either. No experimental structures have been reported yet.

(34) Li, J.; Pyykkö, P. *Inorg. Chem.* **1993**, *32*, 2630.

Table 6. Additional Geometric Parameters of the Carbon-Centered Systems (in pm and deg)

system	variable	method	value
CH_3AuL	C−H bond	HF	109.27
		RI-MP2	110.05
		MP2	110.05
$CH_2(AuL)_2$	C−H bond	HF	109.37
		RI-MP2	110.11
		MP2	110.12
$(NC)_2C(AuL)_2$	C−C bond	HF	144.43
		RI-MP2	144.20
		MP2	144.22
$(NC)_2C(AuPPh_3)_2$		expt[48]	143.5
	N≡C bond	HF	113.91
		RI-MP2	118.38
		MP2	118.38
$(NC)_2C(AuPPh_3)_2$		expt[48]	115
	C−C−C angle	HF	112.16
		RI-MP2	115.92
		MP2	115.89
$(NC)_2C(AuPPh_3)_2$		expt[48]	113.4
$CH(AuL)_3$	C−H bond	HF	109.38
		MP2	110.00
		RI-MP2	109.98
	H−C−Au angle	HF	110.58
		MP2	122.03
		RI-MP2	122.21
$Me_3PC(AuPPh_3)_3^+$		expt[49]	116.8
$CH(AuL)_4^+$	C−H bond	HF	109.38
		RI-MP2	110.70
	H−C−Au angle	HF	104.73
		RI-MP2	110.15
$Me_3PC(AuPPh_3)_3^+$		expt[36]	111

The protonated species $CH(AuL)_4^+$ has an MP2 structure in excellent agreement with the experimental $CH(AuPPh_3)_4^+$ one of ref 35. If the hydrogen is replaced by an sp^2 carbon, as in ref 36, the experimental structure does not change much.

The MP2 proton affinity of $C(AuPH_3)_4$ is 1166 and 1213 kJ/mol starting from the T_d and C_{4v} structures, respectively. All three structures were separately optimized. These numbers are huge, compared to the experimental values of 854 and 543.5 kJ/mol for NH_3 and CH_4, respectively.[37] Our own MP2 proton affinity of NH_3 is 918 kJ/mol. Thus it becomes natural that the compound of Schmidbaur et al. survives in the presence of another strong Lewis base, such as dimethylaniline[35] (proton affinity 941 kJ/mol). In the NIST database,[37] only certain alkali metal and alkaline earth oxides possess gas-phase proton affinities above 1200 kJ/mol.

The $C(AuL)_5^+$ species appears to prefer trigonal bipyramidal C_{3v} (distorted D_{3h}) symmetry over the C_s (C_{4v} for the C−Au core) by a very small, 2.5 kJ/mol, margin. The calculation agrees with experiment here. The calculated bond lengths are slightly below the experimental values.

The $C(AuL)_6^{2+}$ structure is determined by the octahedral framework symmetry. The MP2 C−Au is 207.3 pm, compared to the experimental 212.5 pm.

The "gilded ammonia", $N(AuL)_3$, also strongly decreases its Au−N−Au angle due to correlation. Its MP2 proton affinity becomes 1125 kJ/mol, suggesting that this system also is a strong Lewis base. The experimental structures where the N−H bond is replaced by N−C or N−O bonds agree well with the MP2 one.

The $N(AuL)_4^+$ T_d structure lies 54 kJ/mol below the C_{4v} one. No C_{3v} minimum was found.

The calculated $O(AuL)_3^+$ geometry is flat at the HF level, and its Au−O−Au angle shrinks to 94.6 at the MP2 level, compared to 91.3 for $N(AuL)_3$. The compound of Nesmeyanov et al.[38] is dimeric. That of Angermaier and Schmidbaur[39] is monomeric but has bulky phosphines. These differences might explain the larger deviations of the experimental angles from the calculated ones.

The $O(AuL)_4^{2+}$—the gold analogue of the doubly protonated water molecule—complex has a structure computationally very similar to the crystallographic one. Estimates of aurophilic contribution to its stability (see details below) give a value of 18.3 kJ/mol per Au−Au pair, or 108 kJ/mol per ion.

The $S(AuL)_2$ bond angle as a function of the method was compared with the experiment in Figure 2. The analogous $S(CuL)_2$ systems have been studied by Ahlrichs et al.[40]

$S(AuL)_3^+$ has been studied earlier[41] with a smaller basis set and only partial geometry optimization. The current results, with a larger Au basis and a 19-VE ECP, give an Au···Au distance and an Au−S−Au that are smaller than those in ref 41 and considerably below the experimental values. On one hand, as seen in Figure 2 for the neutral A-frame, the MP2 level exaggerates the aurophilic attraction. On the other hand, as pointed out in ref 41, the wider bond angles in the experimental system may be caused by steric effects between bulky ligands, which are increasing the otherwise unusually small (82°) Au−S−Au angles.

The $S(AuL)_4^{2+}$ C_{4v}, C_{3v}, and T_d relative MP2 energies are 0, +49, and +52 kJ/mol. This order rationalizes for the first time the observed[29] C_{4v} structure for $S(AuPPh_3)_4^{2+}$.

The phosphonium ion $P(AuL)_4^+$ has three MP2 minima, C_{4v}, C_{3v}, and T_d at 0, +68, and +77 kJ/mol, respectively. As predicted earlier by Li and Pyykkö,[34] the tetrapod lies lowest. No clear-cut experimental analogues exist.[42] The proton affinity of this species, C_{4v} to C_{4v}, is 663 kJ/mol. One experimental compound, with a P−C(aromatic) bond instead of the P−H one, is known,[43] and its structure is close to our MP2 structure.

Comparisons with Free Dimers and Systems with Longer Bridges. In the former parts of this series,[3−5] free dimers and ring systems were studied. For the free dimers, the minima on the Au···Au potential energy curves were found to be typically in the 300−340 pm range, and their interaction energies, relative to infinite separation, were typically smaller than 25

(35) Schmidbaur, H.; Gabbaï, F. P.; Schier, A.; Riede, J. *Organometallics* **1995**, *14*, 4969.
(36) Scherbaum, F.; Huber, B.; Müller, G.; Schmidbaur, H. *Angew. Chem.* **1988**, *100*, 1600; *Angew. Chem., Int. Ed. Engl.* **1988**, *27*, 1542.
(37) The NIST standard reference database: http://webbook.nist.gov/chemistry/, 1997.
(38) Nesmeyanov, A. N.; Perevalova, E. G.; Struchkov, Y. T.; Antipin, M. Y.; Grandberg, K. I.; Dyadchenko, V. P. *J. Organomet. Chem.* **1980**, *210*, 343.
(39) Angermaier, K.; Schmidbaur, H. *Acta Crystallogr.* **1995**, *C51*, 1793.
(40) Dehnen, S.; Schäfer, A.; Ahlrichs, R.; Fenske, D. *Chem. Eur. J.* **1996**, *2*, 429.
(41) Pyykkö, P.; Angermaier, K.; Assmann, B.; Schmidbaur, H. *J. Chem. Soc., Chem. Commun.* **1995**, 1889−1890.
(42) Sunic, D. L.; White, P. S.; Schauer, C. K. *Angew. Chem.* **1994**, *106*, 108.
(43) Schmidbaur, H.; Zeller, E.; Weidenhiller, G.; Steigelmann, O.; Beruda, H. *Inorg. Chem.* **1992**, *31*, 2370.

Table 7. Main Geometric Parameters of the Nitrogen-Centered Systems (in pm and deg)

system	method	N−Au bond	Au···Au distance	Au−P bond	Au−N−Au angle	N−Au−P angle
NH_2AuL	HF	202.5		234.6		177.0
	MP2	198.0		227.4		176.0
NH_3AuL^+	HF	217.8		236.1		180.0
	MP2	209.4		227.3		180.0
$NH(AuL)_2$	HF	200.8	347.0	234.1	109.5	177.1
	RI-MP2	199.2	292.2	227.1	94.3	176.1
$NO_2PhN(AuPPh_3)_2$	expt[50]		303			
$NH_2(AuL)_2^+$	HF	211.5	360.0	235.9	116.6	179.4
	RI-MP2	204.6	304.6	227.3	96.2	179.7
$NO_2PhNH(AuPPh_3)_2^+$	expt[50]	220	304	226		
$N(AuL)_3$	HF	199.6	338.6	233.4	116.1	177.5
	RI-MP2	201.0	288.8	227.2	91.9	175.9
$NH(AuL)_3^+$	HF	208.2	344.9	235.6	111.9	179.8
	RI-MP2	201.4	306.9	227.2	99.3	178.7
$NO_2PhN(AuPPh_3)_3^+$	expt[50]		307		89	
c-Hex-$NHC_3H_6N(AuPPh)_3^+$	expt[51]	203	308.8	223.6	99	175
$(Me_3SiO)N(AuPPh_3)_3^+$	expt[52]		312.3		99.8	174.7
$N(AuL)_4^+$ (T_d)	HF	206.0	336.5	235.2	109.5	180.0
	RI-MP2	198.1	323.4	227.1	109.5	180.0
$N(AuL)_4^+$ (C_{3v})						
$N(AuPPh_3)_4^+$	expt[27]	203[a]	344[b]	235[c]		
		201[d]	310[d]			
$N(AuPPh_3)_4^+$	expt[28]	205[a]	334.5[b]		113.0[b]	
		200.5[d]	322.7[d]		105.6[d]	
$N(AuL)_4^+$ (C_{4v})	HF	209.8	296.8	234.8	90.00	179.9
	RI-MP2	208.2	277.2	227.3	83.44	173.7
$N(AuL)_5^{2+}$ (C_{3v})	HF	220.5[a]	306.6[e]	236.8[a]	120.0[e]	180.0
		213.0[f]	368.9[g]	236.68[f]	90.0[g]	
	RI-MP2	208.5[a]	291.1[e]	227.5[a]	120.0[e]	180.0
		203.2[f]	352.0[g]	228.2[f]	90.0[g]	
$N(AuPPh_3)_5^{2+}$	expt[32]	211.4[a]	295.9[g]	224.6[a]	109.6 to	
		206.6[f]		224.5[f]	129.0[g]	
$\{[N(AuPMe_3)_5][Me_3PAuCl]_2\}^{2+}$	expt[53]	212.5[a]	297.0[e]			
		207.7[f]	358.3[g]			

[a] Axial. [b] Axial to nonaxial. [c] Average. [d] Nonaxial. [e] Axial to equatorial. [f] Equatorial. [g] Between two equatorial Au atoms.

Table 8. Main Geometric Parameters of the Oxygen-Centered Systems (in pm and deg)

system	method	O−Au bond	Au···Au distance	Au−P bond	Au−O−Au angle	O−Au−P angle
OHAuL	HF	200.4		231.5		177.3
	MP2	194.9		223.3		176.9
OH_2AuL^+	HF	225.0		234.9		179.3
	MP2	208.8		224.6		178.0
OH_3AuL^{2+}	HF	dissociates into OH_3^+ and AuL^+				
	MP2	dissociates into OH_3^+ and AuL^+				
$O(AuL)_2$	HF	197.3	350.2	230.6	125.1	177.2
	RI-MP2	195.5	295.7	223.4	98.3	177.4
$OH_2(AuL)_2^{2+}$	HF	248.0	433.3	237.4	121.8	177.1
	RI-MP2	218.6	308.6	226.2	89.8	179.2
$O(AuL)_3^+$	HF	204.8	354.8	232.3	120.0	180.0
	RI-MP2	202.9	298.1	224.8	94.6	176.7
$O(AuPPh_3)_3^+$	expt[38]	197	309.4	226	103	174
$O(AuP\,{}^iPr_3)_3^+$	expt[39]	203.0	319.8	222.8	103.7	176.4
$O(AuL)_4^{2+}$ (T_d)	HF	213.5	348.7	234.2	109.5	180.0
	RI-MP2	203.6	332.5	225.0	109.5	180.0
$O\{Au[P(Ar)_3]\}_4^{2+}$	expt[33]	205.7	335.9	222.5	109.5	180.0

kJ/mol. For the bridged systems, Au···Au distances as short as 260 pm (in $Au_2I_4^{2-}$) were found; no energetic estimates were made, however. In the current study, the Au···Au distances are typically 290−320 pm (unless Au−X−Au angles are fixed by symmetry), with energetic effects up to 100 kJ/mol (see below). It can be concluded that the Au−X−Au bridges behave as mediators of the aurophilic attraction, bringing the gold atoms closer and thus increasing the interaction energy.

4.2. The Aurophilic Energies. A method for assessing the role of the specific correlation effects attributable to the aurophilic attraction in these centered systems is less obvious, because correlation effects also influence the primary chemical bonds as such. We have at least two proposals. One is to compare the changes of the correlation energies in isodesmic reactions which leave the number of primary bonds unchanged. Another is to look for a total-energy increment, dependent on the number and possibly distance of M−M pairs. A broad, general correlation between the attraction, $V(R_e)$, and the secondary, M−M bond length, R_e, was proposed in ref 1 (Chapter II. D., Figure 36).

For the first model, consider a hypothetical chemical reaction that forms a centered system of the type investigated here out of "monomers" containing only one gold atom (and thus no gold−gold interaction). To minimize other effects on the estimate of the aurophilic interaction energy, the reaction should preferably con-

Table 9. Main Geometric Parameters of the Sulfur-Centered Systems (in pm and deg)

system	method	S−Au bond	Au···Au distance	Au−P bond	Au−S−Au angle	S−Au−P angle
SHAuL	HF	235.7		237.6		178.4
	MP2	228.3		228.1		178.9
SH_2AuL^+	HF	247.6		238.6		178.4
	MP2	235.7		229.2		178.5
$S(AuL)_2$	HF	233.6	356.3	236.9	99.4	177.1
	RI-MP2	228.2	291.1	227.3	79.3	178.0
$S(AuPPh_2)_2$	expt[54]	215.9	301.8	213.5	88.7	176.5
$S(AuL)_3^+$	HF	238.8	377.5	238.0	104.4	176.6
	RI-MP2	233.1	294.4	228.6	78.3	176.3
$S[AuP(iPr)_3]_3^+$	expt[55]	228.5	325.3	224.0	90.8	169.9
$S(AuL)_4^{2+}$ (T_d)	HF	243.7	397.9	238.6	109.5	180.0
	RI-MP2	230.9	377.0	229.3	109.5	180.0
$S(AuL)_4^{2+}$ (C_{3v})	HF			changes into T_d		
	RI-MP2	233.0[a]	417.6[b]	228.5[a]	128.1[b]	180.0[a]
		231.4[c]	315.5[c]	229.1[c]	85.9[c]	179.6[c]
$S(AuL)_4^{2+}$ (C_{4v})	HF	247.9	329.3	239.0	83.2	174.2
	RI-MP2	238.9	284.5	229.8	73.1	172.8
$S(AuPPh_3)_4^{2+}$	expt[29]	239.9	291.0	227.0	74.7	174.6

[a] Axial. [b] Axial to equatorial. [c] Equatorial.

Table 10. Main Geometric Parameters of the Phosphorus-Centered Systems (in pm and deg)

system	method	$P_{cent.}$−Au bond	Au···Au distance	Au−$P_{lig.}$ bond	Au−P−Au angle	P−Au−P angle
PH_2AuL	HF	240.9		244.1		177.9
	MP2	234.6		234.1		177.4
PH_3AuL^+	HF	242.3		242.3		180.0
	MP2	233.1		233.1		180.0
$PH_2(AuL)_2^+$	HF	241.4	426.1	242.3	124.0	179.0
	RI-MP2	232.0	390.5	232.9	114.6	179.9
$PH(AuL)_3^+$	HF	240.8	404.1	242.3	114.1	179.4
	RI-MP2	230.5	375.0	232.8	108.9	179.4
(*o*-Tol)$P(AuPPh_3)_3^+$	expt[56]	230.5	368.1	229.4	106.0	175.0
$P(AuL)_4^+$ (T_d)	HF	239.8	391.6	242.2	109.5	180.0
	RI-MP2	229.2	374.4	232.4	109.5	180.0
$P(AuL)_4^+$ (C_{3v})	HF			turns into T_d		
	RI-MP2	229.0[a]	416.5[a]	230.7[a]	129.9[a]	180.0[a]
		230.7[b]	306.4[b]	231.8[b]	83.2[b]	177.5[b]
$P(AuL)_4^+$ (C_{4v})	HF	246.5	310.5	242.7	78.1	171.8
	RI-MP2	240.7	278.9	232.3	70.8	170.9
$PH(AuL)_4^{2+}$ (C_{4v})	HF	247.3	337.5	242.0	86.1	177.0
	RI-MP2	234.5	295.6	232.9	78.1	177.65
(*o*-Tol)$P(AuPPh_3)_4^{2+}$	expt[43]	236.7	296.7	229.3	77.6	176.6

[a] Axial. [b] Nonaxial.

serve the number and character of chemical bonds involved, i.e., be isodesmic. For example, a carbon-centered A-frame could be studied on the basis of the following reaction:

$$2CH_3AuL \rightarrow CH_2(AuL)_2 + CH_4 \qquad (2)$$

For charged systems, the count of individual charges should also be preserved, e.g.,

$$NH_3AuL^+ + 2NH_2AuL \rightarrow NH(AuL)_3^+ + 2NH_3 \qquad (3)$$

To obtain a measure for the aurophilic attraction energy, the change in the MP2 *correlation* energies in such isodesmic reactions was calculated and divided by the number of Au···Au interactions present in the system (N):

$$E^{(1)} = \Delta E_{corr}^{MP2}/N \qquad (4)$$

The upper index [(1) in $E^{(1)}$] will be used to enumerate the different ways of estimating the aurophilic energy in this work.

Two ways of finding N were used. In the first one, all Au···Au pairs were considered, and the average value for $R_{Au\cdots Au}$ was used in the distance−energy relationships discussed below. In the second one it was assumed that since the gold−gold interaction dies off relatively fast (proportional to R^{-6}), only the closest Au···Au interactions should be included in the N count, and the longer-range ones ignored. The actual Au···Au distance becomes a uniquely defined quantity in this case.

Irrespective of the counting method, an aurophilic attraction was invariably found (Table 11). The majority of the obtained values are in the 40−80 kJ/mol range, with deviations in both directions. When plotting the energy against the Au···Au distance, R, a rough correlation can be observed among the present systems (Figures 3 and 4).

A Herschbach−Laurie type fit,[44] assuming an exponential repulsive interaction and a power-law type ($-r^n$) attraction, was derived in ref 1, eq 24:

$$E^{(2)} = -(Rb/n)(10^2\text{N/m})\exp((R - a)/b) \qquad (5)$$

Table 11. Au···Au Distances (pm) and Aurophilic Interaction Energies (kJ/mol) of the Systems Studied

	Au···Au distance		aurophilic energy		
system	average	closest	$E^{(1)}$ per Au···Au pair	$E^{(1)}$ per closest contact	$E^{(3)}$
$CH_2(AuL)_2$	294.02	294.02	−84.3	−84.3	−29.8
$CH(AuL)_3$	294.64	294.64	−78.8	−78.8	−19.3
$C(AuL)_4(T_d)$	321.61	321.61	−57.6	−57.6	−8.2
$C(AuL)_4(C_{3v})$	320.92	307.44	−58.6	−113.6	−8.3
$C(AuL)_4(C_{4v})$	314.76	276.57	−71.3	−107.0	−9.6
$C(AuL)_5^+(C_{3v})$	319.18	288.28	−43.3	−72.2	−8.4
$C(AuL)_5^+(C_s)$	316.23	287.01	−45.8	−114.5	−9.0
$C(AuL)_6^{2+}(D_{3d})$	317.49	293.2	−37.4	−46.8	−9.0
$NH(AuL)_2$	292.16	292.16	−94.6	−94.6	−31.7
$NH_2(AuL)_2^+$	304.60	304.60	−23.9	−23.9	−28.8
$N(AuL)_3$	288.82	288.82	−93.3	−93.3	−22.5
$NH(AuL)_3^+$	306.86	306.86	−41.4	−41.4	−15.2
$N(AuL)_4^+(T_d)$	323.43	323.43	−38.7	−38.7	−7.0
$N(AuL)_4^+(C_{4v})$	315.43	277.16	−55.5	−83.3	−10.5
$N(AuL)_5^{2+}(C_{3v})$	321.95	291.1	−38.9	−64.8	−7.8
$O(AuL)_2$	295.73	295.73	−99.7	−99.7	−30.2
$OH_2(AuL)_2^{2+}$	308.56	308.56	−16.0	−16.0	−69.1
$O(AuL)_3^+$	298.13	298.13	−48.4	−48.4	−21.8
$O(AuL)_4^{2+}(T_d)$	332.54	332.54	−18.3	−18.3	−9.1
$S(AuL)_2$	291.06	291.06	−90.2	−90.2	−39.0
$S(AuL)_3^+$	294.39	294.39	−56.0	−56.0	−31.0
$S(AuL)_4^{2+}(T_d)$	377.04	377.04	−7.6	−7.6	−10.2
$S(AuL)_4^{2+}(C_{3v})$	366.54	315.51	−16.9	−33.8	−10.6
$S(AuL)_4^{2+}(C_{4v})$	323.80	284.52	−38.5	−57.8	−21.4
$PH_2(AuL)_2^+$	390.47	390.47	−6.5	−6.5	−23.0
$PH(AuL)_3^+$	374.95	374.95	−20.0	−20.0	−12.8
$P(AuL)_4^+(T_d)$	374.35	374.35	−24.6	−24.6	−8.7
$P(AuL)_4^+(C_{3v})$	361.43	306.41	−36.5	−73.0	−10.1
$P(AuL)_4^+(C_{4v})$	317.35	278.85	−58.1	−87.2	−16.9
$PH(AuL)_4^{2+}(C_{4v})$	336.38	295.57	−38.5	−57.8	−17.3

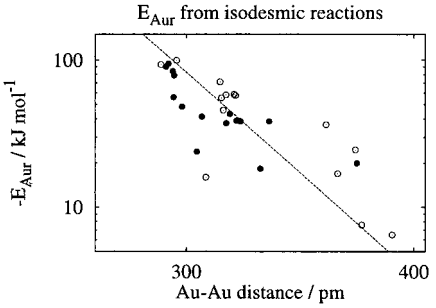

Figure 3. Estimated aurophilic interaction energies $E^{(1)}$ plotted against the average Au···Au distance. All Au···Au interactions are included, and distances are averaged. Filled circles represent experimentally known systems. The straight line represents a Herschbach−Laurie-type relationship with $n = 2.1$.

The Herschbach−Laurie constants $a = 268$ pm and $b = -29$ pm are experimental values from ref 45. Then eq 5 would approximate the energy−distance correlation with $n = 2.1$ if the all-inclusive counting method for N is used, and $n = 2.7$ if only the closest Au···Au contacts are counted (straight lines in Figures 3 and 4). With the poor correlation between the distance and energy, we did not find any reason to prefer one counting method over another one.

It is important to note that the Herschbach−Laurie-type relationships describe the minima on the corresponding potential energy curves and should not be confused with the long-range behavior of the gold−gold interaction. The latter has been found to follow an R^{-6} power law in previous studies.[4]

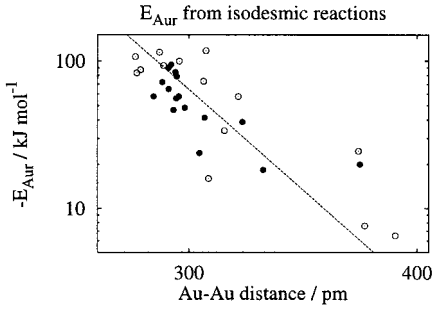

Figure 4. Estimated aurophilic interaction energies $E^{(1)}$ plotted against the shortest Au···Au distance in each given species. Only the shortest-distance Au···Au interactions are included. Filled circles represent experimentally known systems. The straight line represents a Herschbach−Laurie-type relationship with $n = 2.7$.

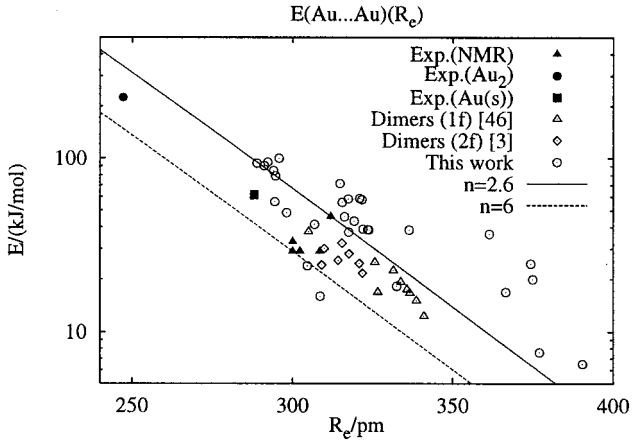

Figure 5. Various experimental and calculated estimates of aurophilic energy, plotted against Au···Au distance.

Thus, using this model, one could estimate the aurophilic energy contribution to the stability of a centered system on the basis of eq 5. The errors remain quite large, however: up to 3 times the calculated values for the worst cases. For the experimentally known systems the deviations are slightly smaller.

Equation 5 can be used to relate the Au−Au interaction energy E, of whatever origin, to the equilibrium Au···Au distance R_e. The results are shown in Figure 5. As seen, the covalently bound Au_2 and metallic Au follow the same trend as the calculated and NMR data for Au(I) interactions. Parenthetically, about one-sixth of the cohesive energy of metallic gold is ascribed to the van der Waals interactions between the d^{10} cores.[47]

(44) Herschbach, D. R.; Laurie, V. W. *J. Chem. Phys.* **1961**, *35*, 458.
(45) Perreault, D.; Drouin, M.; Michel, A.; Miskowski, V. M.; Schaefer, W. P.; Harvey, P. D. *Inorg. Chem.* **1992**, *31*, 695.
(46) Pyykkö, P.; Li, J.; Runeberg, N. *Chem. Phys. Lett.* **1994**, *218*, 133.
(47) Rehr, J. J.; Zaremba, E.; Kohn, W. *Phys. Rev. B* **1975**, *12*, 2062.
(48) Smyslova, E. I.; Perevalova, E. G.; Dyadchenko, V. P.; Grandberg, K. I.; Slovokhotov, Y. L.; Struchkov, Y. T. *J. Organomet. Chem.* **1981**, *215*, 269.
(49) Schmidbaur, H.; Scherbaum, F.; Huber, B.; Müller, G. *Angew. Chem.* **1988**, *100*, 441; *Angew. Chem., Int. Ed. Engl.* **1988**, *27*, 417.
(50) Perevalova, E. G.; Grandberg, K. I.; Smyslova, E. I.; Kuz'mina, L. G.; Korsunskii, V. I.; Kravtsov, D. N. *Metalloorg. Khim.* **1989**, *2*, 1002.
(51) Lange, P.; Beruda, H.; Hiller, W.; Schmidbaur, H. *Z. Naturforsch.* **1994**, *49b*, 781.
(52) Tripathi, U. M.; Scherer, W.; Schier, A.; Schmidbaur, H. *Inorg. Chem.* **1998**, *37*, 174.
(53) Angermaier, K.; Schmidbaur, H. *Inorg. Chem.* **1995**, *34*, 3120.
(54) Lensch, C.; Jones, P. G.; Sheldrick, G. M. *Z. Naturforsch.* **1982**, *37b*, 944.
(55) Angermaier, K.; Schmidbaur, H. *Chem. Ber.* **1994**, *127*, 2381.

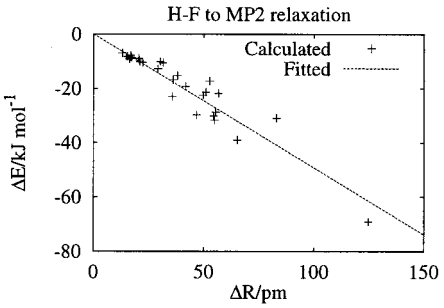

Figure 6. Dependence of the HF to MP2 relaxation energy on change in Au···Au distance.

It can also be seen that the present calculations tend to yield aurophilic interaction energies higher than those expected on the basis of extrapolations from previous experimental and theoretical studies. This can be ascribed to both errors of the model (MP2, combined with two f-functions of gold, is likely to overestimate the interaction) and a possible existence of "assisted aurophilic attraction" in bridged systems such as those considered here. It is not impossible that the central atom would play a role not only in bringing the gold atoms close together but also in participating in the transmission of the interaction with its own electron cloud. Furthermore, the free-dimer calculations included the counterpoise correction for the basis-set superposition error (BSSE), while it is not known how to do this for intramolecular calculations.

Another estimate of the aurophilic attraction energy can be based on the difference between the MP2 (including the Hartree−Fock contribution) energies of a system at Hartree−Fock- and MP2-optimized geometries, respectively, divided by the number of Au···Au interactions present in the system (N):

$$E^{(3)} = (E^{\mathrm{MP2}}_{\mathrm{HF\ geometry}} - E^{\mathrm{MP2}}_{\mathrm{MP2\ geometry}})/N \qquad (6)$$

When plotted against the change in Au···Au distance between these two geometries, a roughly linear relationship is observed (Figure 6).

This quantity can be viewed as the energy released by the system when the geometry is relaxed from HF geometry (which presumably includes no or very little aurophilic effects) to MP2 geometry. The near-linearity observed in Figure 6 is probably due to the roughly linear behavior of the atom−atom interaction potential at moderate Au···Au distances and is not expected to survive if a larger variation of Au···Au distances were available.

Nevertheless, a recipe for estimation of the aurophilic contribution to the stability of a compound can be based on this relationship as follows. Consider an unrestricted $X(AuL)_n$ system, assuming 109.5 bond angles at X. Knowing the primary Au−X bond length and the secondary Au···Au distance, one could calculate the deviation of the latter distance from the undistorted structure. Then, using the correlation formula

$$E^{(4)} = 0.49N(R_{\mathrm{tetrahedral}} - R_{\mathrm{actual}}) \qquad (7)$$

where the $R_{(\mathrm{Au\cdots Au})}$ are measured in picometers, one can estimate the aurophilic energy contribution upon this change in geometry in kJ/mol.

The energy estimates $E^{(1)}$ and $E^{(3)}$ do not correlate well with each other, as can be seen from Table 11. This is expected, since $E^{(1)}$ relates to the actual Au···Au distance in the system, while $E^{(3)}$ relates to the difference in energies in a geometry relaxation process, a part of the interaction. The reference point for $E^{(1)}$ is a system where no Au−Au interaction is present (infinite separation), while for $E^{(3)}$ part of the interaction is included in the Hartree−Fock-geometry reference state (finite separation).

Comparisons with Experiment. NMR determinations of intramolecular activation energies, due to the Au···Au interaction, give results in the range 29−46 kJ/mol (ref 1, Table 5). The corresponding Au···Au equilibrium distances are 300−312 pm. In the present, singly bridged, intramolecular case the Au···Au equilibrium distances can be as short as 278 pm (for $CH(AuL)_4^+$), and hence even larger aurophilic energies can be expected. As seen from Table 11, the largest aurophilic energies are indeed larger than 100 kJ/mol.

A Molecular-Mechanical Model. In the absence of symmetry constraints, the geometry of a centered system is influenced by three distinct forces: the Au···Au attraction, a repulsive term caused by distortion of the framework geometry (such as bending of the Au−X−Au angle from its near-tetrahedral HF minimum), and another repulsive term caused by direct contact of the Au electron clouds. At typical Au···Au distances near 300 pm, one expects all three to affect the geometry of the systems (see also the Au···Au energy curves for free dimers in parts I and II of this series[3,4]).

In the systems where the Au···Au distance is symmetry-constrained (such as the T_d, D_{3h}, or O_h local geometries), the primary factor counteracting the aurophilic attraction is the compression of the primary X−Au bond. Since the repulsive part of a covalent bond is strong, the resulting deformation is very small. Indeed, the systems of high symmetry are clustered in the upper left part of the plot in Figure 6.

The behavior of a potential energy curve influenced by the three above-mentioned factors can be studied by plotting several of these curves as a function of the parameters. In the simple model used for these plots, the Au−Au attraction was modeled by an R^{-6} curve, the Au−Au repulsion at close distances by an R^{-12} curve, and the Au−X−Au bending by a $(R - R_0)^2$ function:

$$E^{(5)} = \left(\frac{1}{R}\right)^{12} - \left(\frac{1.2}{R}\right)^{6} + 5(R - R_0)^2 \qquad (8)$$

A set of the resulting curves, differing only in the value of R_0 in the range 0.6−1.8, is shown in Figure 7. The solid line connects the minima of the respective potential energy surfaces.

Two important features may be noted here: first, there are two possible locations of the minima, depending on the relative strength of the gold−gold attraction and the counteracting bending force. In principle, systems with a bistability, i.e., possessing minima at both the wide-open and narrow configurations, could exist, but no such behavior was found in the systems investigated here. The potential energy surface is also nearly flat in such cases. Second, while the depth of

(56) Schmidbaur, H.; Weidenhiller, G.; Stiegelmann, O. *Angew. Chem.* **1991**, *103*, 442; *Angew. Chem., Int. Ed. Engl.* **1991**, *30*, 433.

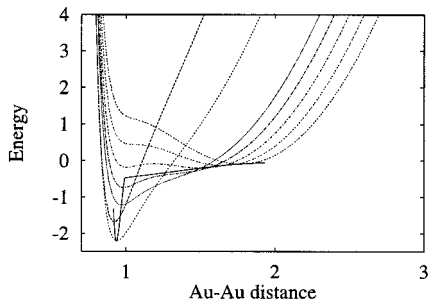

Figure 7. Influence of the relative location of the minima of Au−Au interaction on the shape of the model Au−Au potential. The solid line connects the minima of the respective curves. Units are arbitrary.

the minimum strongly depends on the relative strengths of the counteracting forces, the location of the narrow-angle minimum changes surprisingly little until the sharp transition into the wide-open region occurs.

This may be relevant to the observation that most gold−gold distances in nonsymmetry-constrained molecules are in the region 290−325 pm, with some exceptions in the 375−390 pm range. The latter are $PH_2(AuL)_2^+$ and $PH(AuL)_3^+$, neither of which shows a significant contraction of the Au−Au distance in the transition from HF to MP2. These two systems can thus be expected to represent situations where the attraction is not able to overcome the bending counteraction, and thus the minimum is located in the wide-open region of the potential energy surface (PES). The rest of the systems are representative of the short-range minima. Their depth varies a great deal, while their location is nearly constant.

5. Conclusions

(1) The present MP2 geometries are in fair agreement with experiment but may give Au···Au distances up to 10 pm shorter than the experimental ones. The first more accurate alternative, CCSD, is too costly for a large-scale study like this. Concomitantly, at the MP2 level the interaction energy is somewhat too large.

(2) An isodesmic reaction scheme is used to extract the MP2-level aurophilic attraction energy. At the shortest distances here, values up to 115 kJ/mol per Au−Au pair are found.

(3) The strong Au···Au interactions lead to the huge proton affinity of tetrahedral $C(AuL)_4$. The MP2 value is 1213 kJ/mol. This explains the stability of the recently synthesized[35] $CH(AuPPh_3)_4^+$.

(4) The aurophilic contribution to the stability[33] of $O(AuPPh_3)_4^{2+}$ is estimated as 108 kJ/mol.

(5) The present interaction energies roughly follow the correlation with $R_{Au\cdots Au}$, proposed earlier[1] (Figure 5).

Acknowledgment. This work was supported by The Academy of Finland. The calculations were performed on DEC Alpha Station 500/500 workstations of this laboratory as well as in the Center of Scientific Computing in Espoo, Finland. We are grateful to the group of Prof. R. Ahlrichs (University of Karlsruhe) for providing us with the Turbomole package capable of performing RI-MP2 calculations.

OM980255+